Droplet Radiator Systems for Spacecraft Thermal Control

Robert T. Taussig*
Spectra Technology, Incorporated,†Bellevue, Washington
and
A. T. Mattick‡
University of Washington, Seattle, Washington

Liquid-droplet radiators (LDRs) can be as much as 5 to 10 times lighter than advanced heat pipe radiators. They are virtually immune to puncture, stow in a small volume, and are easily deployed. Systems studies show that they optimize in the 10- to 100-MW size for liquid lithium, tin, and aluminum and at several hundred kilowatts for NaK and vacuum oils. Larger radiators can be constructed from modules of these sizes. Power systems reoptimized for the light LDR mass operate at 100 K lower reject heat temperatures and may be 3 to 5 times lighter than those using conventional radiators. Recent collector tests have revealed a splash-free regime of operation promising high collection efficiencies. LDR tests in space should be feasible in the near future.

Nomenclature

A = radiator sheet area (one side)
A_r = radiator aspect ratio
Bo = Bond number of rotating collector film
c = droplet liquid specific heat
C = evaporation rate function
d = separation distance between adjacent droplet streams
E_3 = elliptic integral
F_r = Froude number of rotating collector film
L_r = length of radiator sheet
$\dot{m}_e$ = droplet sheet evaporation rate per unit area
$\dot{m}_f$ = droplet sheet mass flow rate
M = total mass of droplet sheet radiator
M_f = mass of droplets in flight
P, P_r = radiated thermal power
r = droplet radius
Re = Reynolds number of rotating collector film
s = droplet sheet thickness
T_0 = radiator inlet temperature
T_1 = radiator outlet temperature
T_e = effective mean radiator temperature
T_{peak} = peak thermal cycle temperature
u = droplet velocity
u_r = radial flow velocity of rotating collector film
U_θ = tip velocity of rotating collector
w = droplet sheet width at droplet generator
We = relative droplet Weber number
β = evaporated mass fraction
ϵ_0 = intrinsic emissivity of droplet liquid
$\epsilon, \epsilon_{sheet}$ = mean hemispherical emissivity of droplet sheet
λ = separation distance between droplets in a single stream
ρ = droplet liquid mass density
ρ_a = droplet sheet area density (kg/m^2)
σ = Stefan-Boltzmann constant
τ, τ_{sheet} = mean optical depth of droplet sheet
τ_0 = optical depth of droplet sheet at droplet generator
τ_L = radiator lifetime
ω = angular velocity of rotating collector

Presented as Paper 84-1797 at the AIAA 19th Thermophysics Conference, Snowmass, CO, June 25-28, 1984; submitted Oct. 1, 1984; revision received April 1, 1985.

*Director of Energy Technology. Member AIAA.
†Formerly Mathematical Sciences Northwest, Inc.
‡Research Associate Professor, Aeronautics & Astronautics.

Introduction

SMALL liquid droplets offer a very lightweight way to reject waste heat from space power systems because of their high surface area per unit mass. Lightweight radiators will become a necessity as the need for higher powers in space increases. Missions are now under consideration that will require rejection of megawatts of waste heat on a continuous basis, and future missions may need to reject hundreds to thousands of megawatts. The very feasibility of such missions is brought into doubt because conventional radiators are too heavy and too difficult to deploy or assemble in space.

Liquid-droplet radiators (LDRs) have been investigated by a number of authors[1-5] and have a number of distinctive advantages in this context:

1) The radiating surface is invulnerable to puncture by small particles and by directed energy weapons.

2) They are lightweight because very little fluid mass is required for a given radiating area and armoring against puncture is not required.

3) They can be deployed easily by using a mast that expands to its full length in orbit.

4) They can be stowed in a small volume, such as a canister of liquid and a collapsible structure.

5) They can operate for a long period of time over an appropriate temperature interval where evaporative losses are minimal.

Droplet radiators are still in the conceptual stage of development. Initial experiments exploring the formation of droplets, splashing in simulated zero-G conditions, and radiative cooling from selected droplet materials have been carried out, and an investigation of droplet collector technology, described below, has recently been completed. Preliminary systems analysis of the droplet radiator has accompanied these investigations to guide the experimental endeavors and to model the performance (e.g., total system weight, peak power, radiator effectiveness) of various configurations. The systems model includes each of the major radiator components, such as pumps, nozzle arrays, collectors, and structures that are needed to operate this type of radiator. A description of the systems model and a summary of the major conclusions of that analysis are discussed here.

The LDR Concept

Mattick and Hertzberg have described the basic radiator physics of the liquid-droplet radiator.[1,2] In their model the droplets form a thin sheet with variable optical thickness, depending on the droplet number density, droplet size, and

sheet thickness. The radiative transfer equation was solved assuming isotropic scattering and a constant temperature from top to bottom of the sheet. The only temperature variation considered was in the direction of the droplet velocity due to radiative cooling en route to the collector. Figure 1 shows a triangular droplet sheet radiator with a rotating collector at the focal point.

At the extreme limit of low droplet density (or a very thin sheet), the droplets radiate their heat independently of each other; this is the lightest-weight version of the droplet radiator but also the largest in area. For high droplet densities, the optical thickness increases and radiation from the droplets near the center of the sheet is occluded by neighboring droplets so that the radiative effectiveness of individual droplets decreases. However, the equivalent emissivity of the droplet sheet increases so that the required sheet area decreases. For optical depths much greater than 4 or 5, a point of diminishing returns is reached where the sheet becomes heavier without real gain in emissivity. The optical depth τ is defined as $\tau = \pi r^2 S/(d^2\lambda)$. In the case of liquid metal droplets, the sheet emissivity can be larger than the intrinsic material emissivity (i.e., 0.1 to 0.15 in the infrared and near-infrared spectrum) because radiation from the interior droplets escapes via multiple reflections from neighboring droplets. In the case of oils, the droplet emissivity is already high (i.e., 0.5 to 0.85) so that even though radiation from the interior is occluded, the sheet still has a high effective emissivity due to the intrinsic emissivity of the droplet material.

The basic LDR concept relies on the formation of uniform droplets using technology related to ink jet printers. Uniformity of droplet size and velocities ensures equal cooling during droplet travel. Although droplets on the outer edge of the sheet will cool faster than those on the inside, our preliminary calculations indicate that this effect is modest. Analysis of the electric charge induced on the droplets by the space plasma and by solar photon bombardment show that deflection of droplet trajectories due to coulombic repulsion will be small under nearly every conceivable circumstance in near-Earth orbits. On the other hand, atmospheric drag on smaller droplets may prevent such radiators being used for orbital altitudes of less than 250 miles.

A possible deployment sequence for LDRs is shown in Fig. 2. In this sequence, a payload plus power system (e.g., a nuclear reactor) and radiator are launched in the shuttle bay. Calculations by Hertzberg and his co-workers have suggested that up to 10 M Watt of power may be included in one shuttle launch by using the SP-100 technology and a droplet radiator.[6,7] Once separated from the shuttle, a chemical rocket raises the payload to orbit, where the radiator mast untwists from its stowed form and cables snap into place to provide structural rigidity. This configuration shows two parallel triangular droplet radiators; the second radiator sprays the liquid collected at the far end of the first radiator back to the power system for reheating to avoid a heavy return pipe.

LDR Systems Model

A preliminary systems model of a triangular liquid droplet sheet radiator has been developed which incorporates individual models of each of the major components and calculates self-consistently the liquid flow rate, pressure, and component mass at each station in the system. As a consequence, the component sizes and operating conditions are matched throughout the system.

The initial radiator configuration and major components are shown in Fig. 3. The heat exchanger has not been incorporated in the model since it depends on the specific mission and power system used.

Droplet Sheet Model

The main assumptions underlying the droplet sheet calculations are that 1) material is lost primarily through evaporation and aiming inaccuracies; 2) the radiator retains 100% of its load capacity for a given lifetime τ_L (years); and 3) the liquid droplet temperature at the collector is very close to freezing. The input parameters are total radiated power (or peak temperature), droplet material properties (i.e., density, surface tension, viscosity, specific heat, and intrinsic emissivity), optical depth of the sheet, sheet aspect ratio (i.e., = width/length), radiator lifetime, aiming accuracy, droplet radius, and number of radiators operating in parallel. If the total power radiated and number of parallel radiators are input data, a separate calculation must be made of the peak (inlet) temperature of the droplets. The evaporation rate depends on the radiator temperatures and on the optical depth of the sheet: $m_e = [1 - 2E_3(\epsilon_0\tau)]C(T_0, T_1)$, where the factor in square brackets represents the reabsorption of evaporated material by neighboring droplets in the sheet. The factor $C(T_0, T_1)$ increases rapidly with temperature and depends on the droplet material chosen.[8] Each liquid can be used only over a specific range of peak temperatures before evaporation severely limits the lifetime of the radiator.

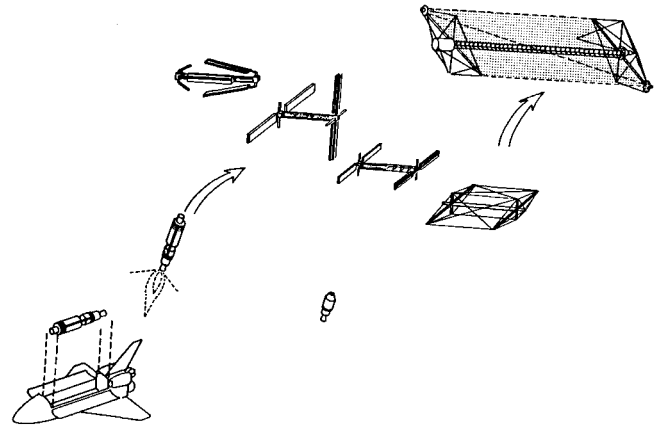

Fig. 2 LDR deployment sequence.

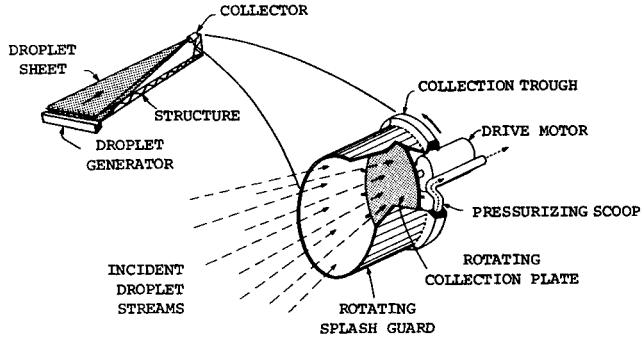

Fig. 1 Triangular LDR with a rotating collector.

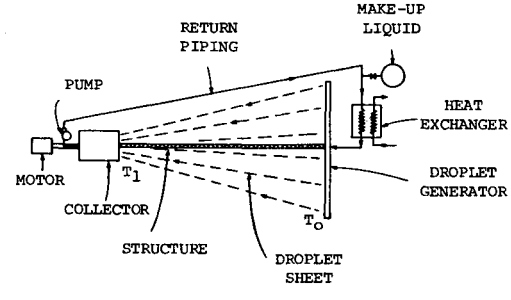

Fig. 3 Droplet radiator systems model.

The following set of equations governs the basic model of the LDR sheet:

In-flight mass: $$M_f = \left[\frac{L}{u}\right]\left[\frac{P_r}{c\Delta T}\right]$$

where $\Delta T \equiv T_0 - T_1$

Evaporation loss: $$2\dot{m}_e \tau_L A = \beta M_f$$

Radiator area: $$A = WL/2 = 0.5 A_r L^2$$

Radiator length: $$L \equiv ut = 2u\tau c r \rho \Delta T / 3\epsilon\sigma T_e^4$$

where $T_e = T_0[3/(f^3 + f^2 + f)]^{1/4}$ and $f = T_0/T_1$

Mass flow rate: $$\dot{m}_f = (4/3) r u \rho \tau_0 A_r L$$

The first equation defines the in-flight mass M_f in terms of the time it takes a droplet to traverse the length L of the radiator (droplet velocity u), and the mass flow rate given by the total power radiated in a single radiator P_r divided by the heat loss per unit mass of the droplets in flight. The second equation relates the evaporation rate $\dot{m}_e$, radiator lifetime τ_L, and surface area of the radiator to the fraction β of the in-flight mass which evaporates over the radiator lifetime. The factor 2 accounts for losses from both sides of the droplet sheet. The third equation defines the radiator area in terms of the radiator length and the aspect ratio A_r. The fourth equation states that the power radiated while the temperature drops from T_0 to T_1 during the droplet's passage from the injector to the collector is equal to the total heat lost from the droplets. The temperature T_e is the average radiation temperature during the droplet's flight ($T_e^4 \equiv <T^4>$). The fifth equation relates the mass flow to the droplet velocity and the density of droplet streams (via τ_0) at the droplet injector. The parameters τ and ϵ are the average optical depth and emissivity of the droplet sheet; τ_0 is the optical depth of the sheet at the injector.

Injector Model

Jet breakup into droplets is assumed to occur in approximately 4.5 nozzle diameters, leading to a droplet radius about twice the nozzle radius. The total number of orifices is related directly to the total power radiated, the mass flow, the droplet size, temperature, and droplet material properties. The height of the droplet sheet and, hence, the height of the injector is related to the droplet size, optical depth, and number density of the droplets in the radiating sheet. Specifying the optical depth and droplet size determines the product of the height of the droplet sheet and the droplet number density in the sheet. Practical consideration of how close nozzles can be placed to each other and/or the number of droplet collisions allowed in transit will govern the upper bound of the droplet number density n.

The flow rate through each nozzle can be expressed in terms of the fluid pressure, the density, and an orifice parameter. A little pressure is lost as the fluid moves along the injector manifold toward the more distant orifices. By tapering the manifold uniformly, the flow velocity can be computed at each orifice; the assumption is made that the droplet velocity at the top (or bottom) of the manifold will be equal to 98% of the droplet velocity at the midplane.

Once the fluid velocity and manifold diameter are known, the total pressure drop and, hence, peak pressure and dimensions of the main manifold can be computed, leading to an estimate of the mass of fluid in the injector, thickness and mass of the injector casing, and mass of the support structure needed to stiffen this component for a desired aiming accuracy. The stiffness requirement remains to be evaluated in detail, but a crude estimate has been made on the basis of the bending modes of a truss beam.

Pipe and Pump Model

The LDR system shown in Fig. 3 relies on a return pipe and a pump. The pump was modeled after liquid metal centrifugal pumps used in the nuclear reactor industry. Typically, these are large (e.g., 17,000 gal/min) and will handle relatively high pressures (e.g., up to 100 or 200 atm). They are driven by electric motors, which constitute 80% of the total pump mass. The entire unit is hermetically sealed. The pump efficiencies on-design can be on the order of 85%. The mechanical portion of the pump was assumed to be 20% of the conventional pump weight. If the conventional motors are replaced by samarium-cobalt permanent magnet motors, the total pump mass will drop significantly since these devices can be designed for high input powers (tens of megawatts) and will weigh on the order of 0.1 lb/kW.

The total mass of the pump, pipe, and coolant filling the pipe is minimized in this model by varying the pipe diameter. For large diameters the pumping power is quite low but the fluid inventory and pipe mass are substantial; for small diameters the pump power and pump mass become very large.

Collector

Several features have been modeled for the rotating collector. This device uses centrifugal force to transfer fluid collected from the droplets to the periphery of the collector, where the fluid is scooped up by a stationary pipe inserted into a trough formed in the cylindrical splash guard surrounding the collector (see Fig. 1). The radius of the collector depends directly on the radiator length and on the aiming accuracy of the droplet injector. The radius is required to be large enough to reduce aperture losses to a level at which the radiator will still operate at full capacity at the end of τ_L years (with βM_f make-up mass). Specific features of the collector model include:

1) Scoops: a model relating the time it takes a fluid layer to refill behind a scoop to the time it takes a scoop to move to the position of the scoop in front of it.

2) Hydraulics: a hydraulic model for liquid layer flow speed and layer thickness on the inner surface of the rotating collector shell.

3) Stability: a model for the normal modes of a combined system consisting of a thin liquid layer and a "flexible" rotating cylindrical shell.

4) Shell design: a model of a honeycomb shell with sufficient stiffness to resist the dominant unstable shell-film mode.

5) Mechanical design: a model of the external structure to contain the rotating collector shell, provide guide wheels on the exterior surface, permit tracking of the incident droplets during orbital maneuvers by the spacecraft, and maintain rotation of the shell.

Structure

The driving forces for attitude control must overcome the gravitational torques either in a periodic or a continuously active mode of adjustment. These adjustments will produce stresses on the structure and will cause it to vibrate at a variety of fundamental frequencies. The normal mode analysis of the truss structure assumes that one end is pinned and computes the stretch mode, torsion mode, free-bending mode, purely translational mode, and purely rotational mode for a massless beam with the collector mass located at the other end of the beam. A finite-mass beam associated with pure buckling was also examined. The fundamental frequencies of each of these modes are computed to determine those conditions under which the longitudinal and transverse vibration frequencies are both higher than the longeron mode. This condition helps to guarantee that the longeron modes will not be excited by the truss modes so that the cross-brace strength will be maintained during maneuvers. The results lead to very light but somewhat flexible trusses.

Computational Results

Calculations based on the LDR systems model have been carried out to determine overall LDR performance. Figures 4 and 5 illustrate variations in the component and total radiator masses as functions of the droplet radius and optical depth for a lithium LDR. In Fig. 4 the initial perception for a fixed radiated power—that the smaller the droplets are, the lighter the radiator will be—is verified for the complete system, at least down to 50-μ size droplets. For example, a threefold reduction in system mass is possible by using 100-μ droplets instead of 500-μ droplets. Figure 5 shows the effect of varying optical depth on the component and total masses of the radiator. The total power radiated also varies, so the power per unit mass P/M is included in this figure. At small optical depths (e.g., $\tau \leq 1$), the droplets are spaced farther apart so that the effective sheet emissivity decreases, requiring a longer, wider radiator (i.e., larger area). A longer radiator requires a higher initial droplet temperature so that the droplets are still above freezing by the time they reach the collector. A higher initial temperature implies an increased evaporation rate and, thus, a larger relative make-up mass is required in order to maintain sufficient lifetime. For large optical depth (e.g., $\tau \geq 4$), the radiator mass again increases faster than the sheet emissivity so that a net increase in mass per unit radiating sheet area occurs.

Both Fig. 4 and 5 show a minimal contribution from the collector mass for the aiming accuracy considered (i.e., 1 mrad). The collector could have a larger diameter than assumed in order to compensate for poorly aimed droplets without compromising the system mass. The collector mass begins to be a significant fraction of the total mass when the aiming accuracy approaches 10 mrad.

The impact of using different droplet liquids has also been evaluated. The resulting performance vs radiated power is shown in Fig. 6 for aluminum, tin, lithium, and Nak. The first three peak near 5 MW, and NaK peaks at about 200 kW. Higher powers may be obtained using multiple radiators. Figure 7 shows performance vs peak temperature, with heat pipe performance (power/mass) shown as a dashed line for comparison (assuming 5 kg/m^2). Lithium, NaK, and DOW 705 oil systems are ~5 to 10 times lighter than heat pipes, whereas aluminum and tin LDRs are not as attractive in this comparison. However, tin and aluminum LDRs return fluid at temperature T_1 that is cooler than the return temperature T_0 of the *constant* temperature heat pipe radiator. Thus, a power cycle could operate more efficiently with the LDR.

A significant variation in the LDR—the use of parallel radiators—has been incorporated in some of the LDR computer studies (e.g., DOW 705 in Fig. 7). Previously it was found that with a single sheet, the mass of the return pipe and

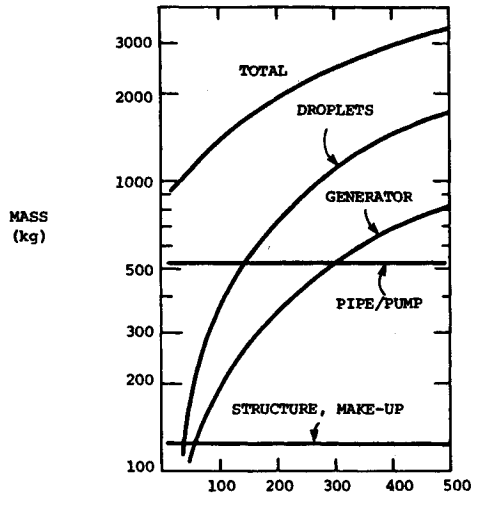

Aiming Accuracy	1 mrad
Lifetime	5 years
Material	Lithium
Optical Depth	3.0
Power	6.3 MW_{th}
Droplet Reynolds No.	2000
Aspect Ratio	0.4
Inlet Temperature	510 K

Fig. 4 LDR component and total mass vs droplet radius.

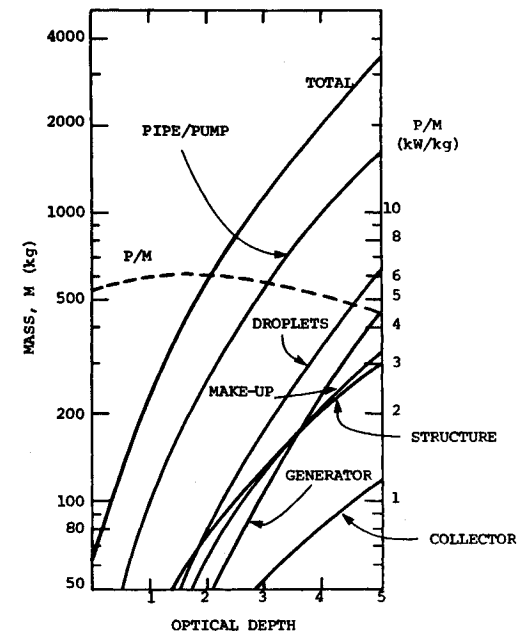

Aiming Accuracy	1 mrad
Lifetime	5 years
Material	Lithium
Droplet Radius	50 microns
Droplet Reynolds No.	2000
Aspect Ratio	0.4
Inlet Temperature	510 K

Fig. 5 LDR component and total masses vs optical depth.

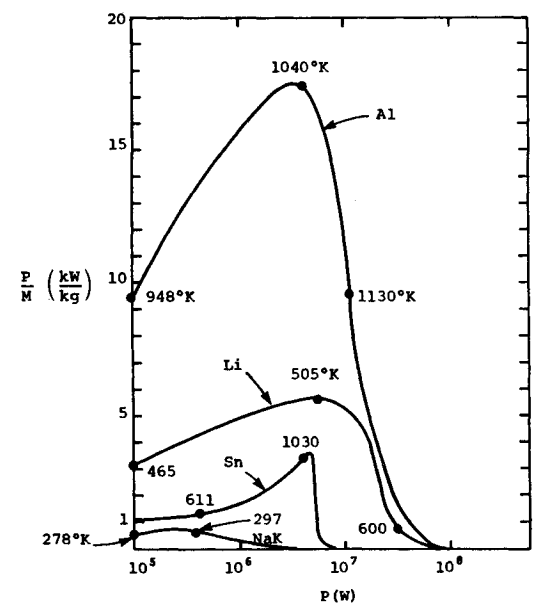

Fig. 6 LDR power/mass vs power radiated.

the pump to overcome pressure losses dominated the LDR system mass for viscous liquids such as silicone oils. Returning the liquid instead by a parallel but oppositely directed sheet has been found to reduce the LDR mass significantly in these cases. Although an additional generator and collector are required, these are downsized since each droplet sheet is smaller than the sheet required for a single traverse.

A point design for a 100 MW_{th} droplet radiator (actually 18 tandem pairs of radiators) has been developed to give a concrete picture of the dimensions and operating parameters for such a device. This design is summarized in Table 1. A large number of streams per radiator ($\sim 10^6$) are required. The in-flight fluid, make-up fluid, and pipe/pump components weigh the most. The power per unit mass of 6.8 kW/kg is nearly 7 times higher than a heat pipe radiator operating at the same effective radiator temperatures ($<T_{rad}>=487$ K). The heat pipe radiator has a higher surface emissivity than the droplet radiator. Since both types of radiators reject the same amount of waste heat, we conclude that the droplet radiator is approximately 7 times lighter than the equivalent heat pipe radiator.

In summary, component models for a triangular sheet droplet radiator have been developed and used in a systems code to evaluate the component masses and total mass of the droplet radiator. The results show that an optimum optical depth, droplet size, and power/mass exist for mission parameters such as total power radiated, radiator temperature, and radiator lifetime. For radiators in the 5 to 100 MW_{th} class, droplet radiators appear to be significantly lighter (by a factor of 7) than the most advanced heat pipe radiators of similar size.

Power Systems Applications

It is worthwhile to reoptimize a thermal power cycle when using a droplet radiator because a more efficient cycle with a lower radiating temperature can be obtained with a potential decrease in the total system mass. We have carried out a reoptimization of two Brayton cycles and a potassium Rankine cycle. The masses of the Brayton cycle components (compressors, turbines, generators, heat exchangers, and recuperators) were scaled from a point design study of a closed-loop, space-based GDL laser power system.[9] Scaling of the heat source and heat sink heat exchangers (most massive components) was carried out from the GDL data according to conventional compact heat exchanger design rules.[10] For a fixed peak temperature, $T_{peak}=1644$K, the remaining cycle parameters were varied to achieve a minimum mass system that would produce 25 MW_e. This optimization was carried out for a range of rejection temperatures of 300 K to 800 K and for several values of radiator specific mass, with and without a recuperator in the cycle.

Table 1 Baseline 100 MW_{th} LDR

Specifications	
Lithium	
5-year lifetime	
Triangular: Base = 33 m	
Length = 83 m	
18 pairs of radiators	
$\epsilon_{sheet}=0.58$, $\tau_{sheet}=3$	
Aiming accuracy = 1 mrad	
Droplet radius = 50 μ	
Droplet speed = 22 m/s	
$T_{in}=528$ K, $T_{out}=460$ K	
Collector radius = 0.33 m	
Pressure drop = 8.5 atm	
Number droplet streams $\cong 3\times10^6$	
Pumping power = 64 kW	
Radiated power = 5.5MW	
Mass radiator	
Structure, kg	1,600
In-flight fluid, kg	2,570
Make-up fluid, kg	4,610
Collector, kg	870
Generator, kg	1,480
Pipe/pump, kg	3,500
	14,630
LDR power/mass: 6.8 kW/kg (Heat Pipe Power/Mass: 1.08 kW/kg) (at $\epsilon=0.85$, $T=487$ K, 5 kg/m^2)	

Figure 8 shows the results of minimizing the mass of the power conversion system plus the waste heat radiator. The radiator mass is estimated by the area density ρ_a, the effective radiator temperature, and the hemispherical emissivity ϵ. The smaller area density of the droplet radiator allows the total system mass minimum to occur at lower cycle temperatures, resulting in a higher-efficiency power cycle and a lighter total power system mass. The thermal cycle efficiency is shown at the minimum of each of the cases illustrated.

The top set of curves corresponds to an advanced heat pipe radiator having an area density of 5 kg/m^2 and an emissivity of $\epsilon=0.85$ for a blackened metal surface. The bottom curves represent a class of possible LDRs having sheet densities of 0.5 kg/m^2 and emissivities corresponding to an optically thick sheet of oil droplets.

Figure 8 also illustrates the potassium cycle results for this analysis. The thermodynamic cycle closely approximates a Carnot cycle in form. While very high-pressure systems (e.g., up to 500 psia) have been considered in the past, we confined our evaluation to 100 psia or lower to ensure longer lifetimes, nearer-term technology, and simpler engineering design. Tabular data taken from Perry[11] and Gruntz[12] have been used to develop analytic approximations to the potassium thermodynamic functions over the temperature and pressure ranges of interest.

The principal components of the Rankine cycle are the heat source heat exchanger (i.e., boiler), the turbine-generators, the heat sink heat exchanger (i.e., condenser), and the radiator. The mass models for the first three components are

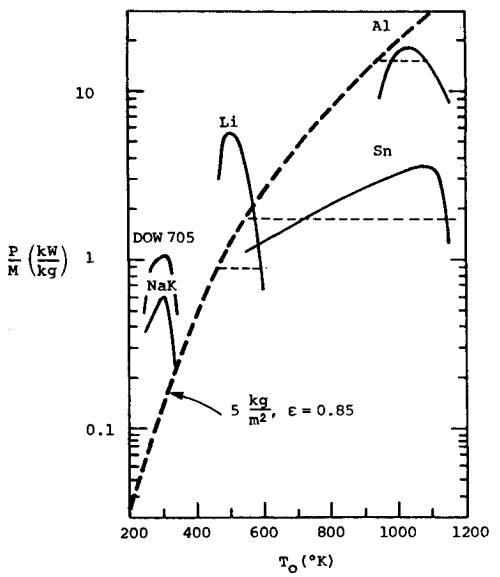

Fig. 7 LDR power/mass vs peak temperature.

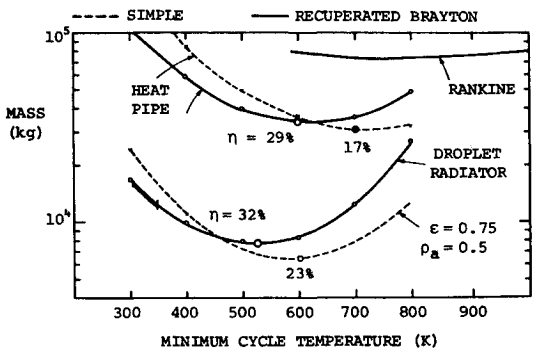

Fig. 8 Reoptimized power cycles.

based on data taken from the design studies for the Solar Power Satellite,[13] which, in turn, draw on the large data base generated during the 1960s and early 1970s for potassium space power systems (for example, see the article by Zimmerman.[14])

A combination of one high-pressure turbine and two low-pressure turbines is used to model the turbine component. Masses per unit electric power generated were taken from Ref. 13 studies and equated to a functional form for the turbine component mass. This function depends on the turbine radius squared and the length or, equivalently, the number of stages per turbine. The turbine radius can be related directly to the square root of the peak cycle temperature divided by the peak cycle pressure and by the work extracted per pound of potassium in the expansion leg of the thermal cycle. The number of turbine stages is related also to the log of the cycle pressure ratio, assuming approximately equal ratios of expansion per stage. The turbine inlet Mach number was assumed constant.

The heat source heat exchanger is a complex assortment of heat absorber tubes, hot manifolds and headers, and the inventory of liquid in these tubes. The potassium boiler component described here also has been modeled in the Ref. 13 studies for several different pressures and temperatures. A chief feature of this component is a strong mass dependence on peak pressures and temperatures. We have modeled this component by relating the boiler mass to the number of tubes needed to transport the potassium at any given flow station and to the tube wall thickness and tube length; the fluid inventory is added to this mass. The number of tubes is taken to be proportional to the total heat input to the system, and the tube wall thickness depends on the peak cycle pressure and on the peak temperature dependence since the creep rupture strength of the piping has a rather strong temperature dependence. This analysis assumes that the actual tube radii will not change from the values used in Ref. 13; a more detailed optimization also should examine the impact of allowing the tube radii to change. The trend toward heavier boilers with increasing peak cycle pressure and temperature is partly, though not very strongly, offset by the increasing cycle efficiency, so that for a given electrical output the amount of heat transferred through the boiler decreases compared to lower pressure cycles.

Since the heat sink heat exchanger is essentially an isothermal condenser at low pressures and moderate temperatures, the tube walls can be much thinner than the boiler tubes. The effectiveness of this component is prescribed in terms of the hot inlet temperature (essentially constant potassium temperature as it condenses) and the cold inlet and outlet temperatures of the radiator coolant. By varying the heat exchanger effectiveness, the mass flow through the radiator can be varied once the radiator liquid specific heat has been fixed.

Calculations using a radiator area density of 5 kg/m^2 show that the radiator is a relatively small fraction of the power system mass in this case. Consequently, one would not expect much benefit to this cycle by descreasing the radiator weight.

The heat source heat exchanger mass is also quite low. The Ref. 13 studies show that this mass does not become significant until peak pressures exceed 200 psia. From 200 to 500 psia, the heat exchanger mass becomes comparable to the turbine mass. The turbine mass actually decreases over this same range of pressures with the sum of heat exchanger and turbine masses remaining nearly constant. Because higher pressures are associated with higher efficiencies, the radiator mass will decrease. Thus, Fig. 8 illustrates a best case so far as the benefits of lighter radiator masses are concerned; it is even harder to show benefits from lighter radiators at higher cycle pressures.

The radiator temperatures favored by this particular cycle are in the range where droplet liquids such as aluminum and tin might be attractive. A slight minimum in the total system mass is shown in Fig. 8 for temperatures near 750 K. The largest power per unit mass ratios for tin droplet radiators occur in the vicinity of a droplet peak temperature of 1030 K (e.g., see Fig. 6), giving a mean effective radiator temperature of approximately 729 K.

These calculations suggest that at least a threefold decrease in power system mass is available for Brayton cycles through the use of liquid-droplet radiators. Also, the mass minima are shifted to lower radiator temperatures compared to the heat pipe radiator cases. This shaft is on the order of 100 K in each case.

Perhaps the most important advantage of droplet radiators is their ability to lower the peak cycle temperature without increasing the system mass compared to one using a conventional radiator. That is, lower peak temperatures will increase the droplet radiator mass since the cycle is less efficient, but the radiator mass is initially so small that it can increase quite a bit before it exceeds the mass of a conventional radiator. For example, a decrease in radiator temperature from 500 to 300 K would permit a drop in peak cycle temperature from 1644 K to 986 K; use of a droplet radiator for the lower temperature cycle would result in the same power system mass as a heat pipe radiator for the higher temperature cycle. This example illustrates the limit of a range of intermediate power cycles that will have both lower peak cycle temperatures and lower system masses than the heat pipe case. From the viewpoint of thermal heat source development, the advantages are truly significant since it is very difficult to gain improvements in the area of high-temperature materials for power systems.[15]

Current Status of Technology

The Air Force and NASA have engaged in a joint program to investigate liquid-droplet radiators. This program is supporting research on droplet generator and droplet materials, radiative transfer from dense clouds of droplets, droplet chargeup in a space environment, droplet radiator systems, and droplet collectors. The droplet generator technology and pump component technologies are the most mature of those needed for droplet radiators. Single streams of uniform droplets can be produced over a wide range of orifice diameters and for a variety of liquids. Single droplet streams can be aimed with better than milliradian accuracies. However, the mechanical control needed to accomplish this same feat with 10^5 to 10^7 droplet streams required for a droplet radiator has not been demonstrated. Up to 1000 streams have been created with uniformly sized droplets in a low-viscosity liquid for ink jet printing. Current laboratory experiments using low-vapor-pressure higher-viscosity oils have recently created on the order of 100 streams from one orifice plate. There is still a considerable challenge to extend this technology to a truly large nozzle array.

A variety of low head pumps have been space-qualified for handling low-temperature fluids in environmental cooling circuits on the shuttle and for cryogenic liquid rocket fuels. The primary zero-G pump requirements for the LDR are to inhibit cavitation at the pump inlet and to provide sufficient inlet pressure to overcome the frictional losses at the pump entrance. Some of these problems have been accentuated for volatile liquids such as the propellants. In these cases, pumps have employed inducers to reduce cavitation. In the case of the liquid-droplet radiator, where very low-vapor-pressure liquids are used, cavitation will not be as serious a problem; rather, the net positive suction head (NPSH), or inlet pressure requirements, will be the key problem area. Laboratory tests of pumps drawing liquid from vacuum vessels have shown that ordinary gear and diaphragm pumps require very little inlet pressurization (e.g., several inches of liquid) for their operation with low-vapor-pressure liquids. Similar pumps have been flight-qualified for low-temperature liquids but not at higher temperatures.

A significant outcome of the LDR systems analysis is that the collector mass can be a large fraction of the system mass unless the aiming accuracy of the droplet generator is better (smaller) than 10 mrad. Consequently, there is a dual urgency

to demonstrate lightweight collector concepts and to verify droplet aiming accuracy in large arrays. Collector efficiency is a key issue. If splashing occurs at a noticeable level at the collector, then liquid may be lost from the system at an unacceptable rate, limiting the lifetime of the mission and possibly contaminating the spacecraft. Collection and splashing experiments have been completed recently for a small rotating collector. Rotation provides an artifical gravity force to fill a trough at the edge of the collector with the incoming droplet liquid (see Fig. 1). A scoop will remove liquid from that trough, pressurizing it for the inlet flow to a low NPSH pump to recirculate the liquid through the waste heat source. Tests of the liquid collection and transport across the rotating collection plate to the trough of the collector have been quite successful. The experimental setup is shown in Fig. 9, which illustrates the vacuum test chamber in the upper left and a closeup of the collector plate and drive motor assembly. Droplet streams are aimed at the collector plate to determine the conditions under which splashing occurred. Various angles of droplet stream impact, different film thicknesses on the rotating plate, different rotation velocities, and a range of droplet sizes and droplet velocities were examined. The results have shown that splashing can be virtually eliminated, within the accuracy of the instrumentation (photographic and visual observation) by operating the droplet stream velocities and plate rotation velocities below a critical relative droplet Weber number. These results are shown in Fig. 10. The splash-free regime corresponds to a range of relative Weber numbers depending on the angle of attack of the droplet stream. This range allows a useful operating range for the LDR system, as shown in Fig. 11, obtained from the LDR systems model for DOW 705. The bars at the top of Fig. 11 compare the range of test dimensionless parameters to those corresponding to a full-scale LDR. (A more detailed discussion of this experiment is published elsewhere.[5]) Additional testing will be required to verify the splash-free regime for denser droplet spray impingement conditions and to demonstrate repressurization of the collected liquid from the trough at the edge of the collector plate.

In addition to component technology development, there are several key system issues that concern the integrated operation of a liquid-droplet radiator. These include component compatibility with the droplet liquid and adjoining elements of the system; integration of the LDR system with the waste heat source; transient and part-load response to the heat source; orbit adjustments and maneuvers (e.g., rapid slewing could result in lost droplets and unbalanced thrusts on the radiator); startup/shutdown conditions; potential spacecraft contamination and droplet liquid contamination by gases from the spacecraft; stowage; and deployment. Very little work has been done to address these issues to date.

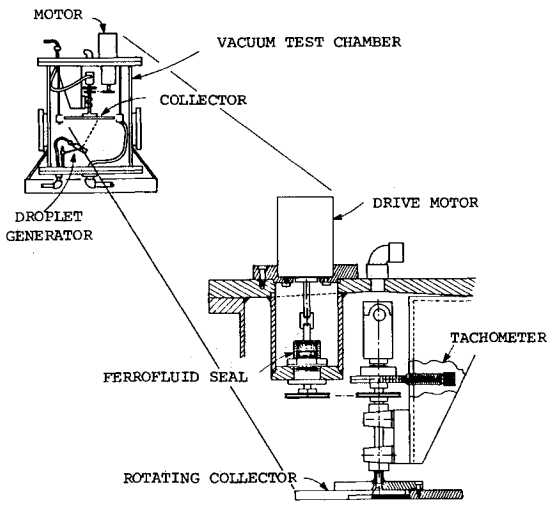

Fig. 9 Test chamber and closeup of rotating collector test equipment.

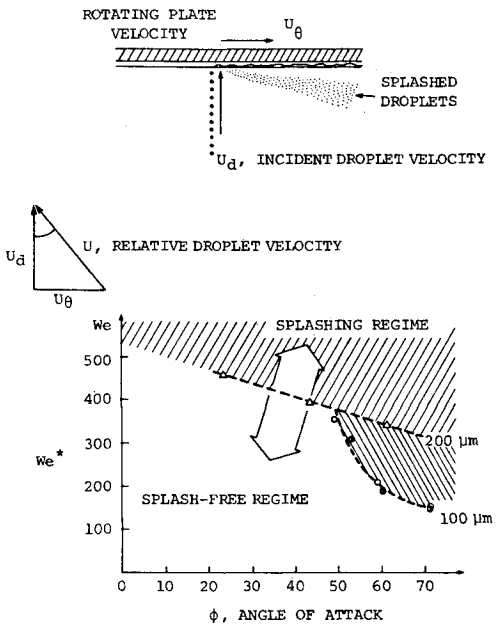

Fig. 10 Relative droplet Weber No. vs ϕ.

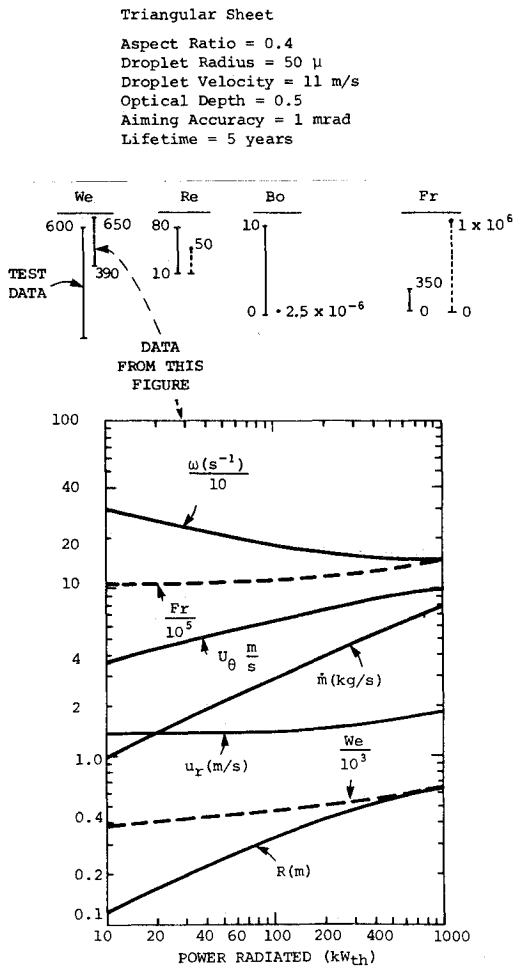

Fig. 11 Rotating collector parameters vs power radiated (DOW 705); bars at top compare test data (left bars) to systems code data (right bars).

Because of the recent success of the collector and droplet generator tests, it seems feasible to demonstrate a scalable version of a droplet radiator for tests in space within the near future. A small LDR could be tested within a suitable enclosure on board the space shuttle. Development of a full-size radiator could follow within a five-year period after these tests, for application to early low-temperature thermal power system or, perhaps, for cryogenic refrigeration systems in space.

Conclusions

Systems analysis has shown that a triangular droplet sheet radiator with a rotating collector can be 5 to 10 times lighter than an advanced heat pipe radiator operating at the same peak temperature. Radiated power per unit mass maxima occur at 5 to 20 MW for liquid lithium, aluminum, and tin and at 100 kW for DOW 705 and NaK. Aiming accuracy and high collection efficiency emerge as critical requirements for LDR performance. Lower radiator weights can lower the total power system mass by a factor of 3 to 5; these mass minima occur at approximately 100 K lower reject heat temperatures compared to heat pipe radiator systems. The low LDR mass also allows the peak cycle temperature (e.g., the nuclear reactor temperature) to be reduced by as much as 40% without increasing the system mass beyond that required for a more conventional heat pipe radiator power system.

Tests of droplet generator and collector concepts have been carried out to measure aiming accuracy, uniform droplet formation, droplet velocity, and collection efficiency. The success of these tests suggests that scalable system demonstrations of the LDR concept can be carried out in the near future, followed by tests in space to verify zero-G performance predictions. Rotating collector test data, in particular, have shown recently that a splash-free regime of operation appears to exist for LDRs using vacuum oils. Further dense droplet stream tests are needed to verify this performance.

Acknowledgment

This work has been supported by the Rocket Propulsion Laboratory at Edwards Air Force Base, California, under Contract No. F04611-81-K-0040.

References

[1]Mattick A. T. and Hertzberg, A. "Liquid Droplet Radiators for Heat Rejection in Space," *Journal of Energy,* Vol. 5, 1981, pp. 387-393.

[2]Mattick A. T. and Hertzberg, A., "The Liquid Droplet Radiator—An Ultralight Heat Rejection System for Efficient Energy Conversion in Space," Preprint IAF-81-185, 32nd Congress of the International Astronautical Federation, Rome, Italy, Sept. 6-12, 1982.

[3]Mattick A. T. and Hertzberg, A., "Liquid Droplet Radiator Technology Issues," Paper TMP-2, First Symposium on Space Nuclear Power Systems, University of New Mexico, Albuquerque, Jan. 11-13, 1984.

[4]Botts, T.E., Powell, J.R., and Horn, F.L., "Magnetic Focusing of Liquid Droplet Sheets for Heat Rejection in Space," Air Force Rocket Propulsion Laboratory Report AFRPLTR-83-072, Dec. 1983.

[5]Mattick A. T. and Taussig, R. T., "New Thermal Management and Heat Rejection Systems for Space Applications," Air Force Rocket Propulsion Laboratory Report AFRPLTR-84-039, June 1984.

[6]Hertzberg, A., "Advanced Lightweight Nuclear Power Sources for Laser Beam Applications," *Proceedings of the 4th GCL Symposium*, Sonesa, Italy, Sept. 1982.

[7]Beals G. et al., "Lightweight Nuclear-Powered OTV Utilizing a Liquid Droplet Radiator," AIAA Paper 83-1346, AIAA/SAE/ASME 19th Joint Propulsion Conference, Seattle, WA, June 1983.

[8]Nesmeyanov, A. N., *Vapor Pressure of the Elements*, Academic Press, New York, 1963.

[9]Young, W. E. and Kelch, G. W., "Closed-Cycle Gas Dynamic Laser Design Investigation," NASA Report No. CR-135130, Jan. 1977.

[10]Kays, W. M., and London, A. L., *Compact Heat Exchangers*, 2nd Ed, McGraw-Hill, New York, 1964.

[11]Perry, R. H., and Chilton, C. H. Eds., *Chemical Engineer's Handbook,* 5th ed. McGraw-Hill, New York, 1973, pp. 3-187.

[12]Robert D. Gruntz, "A Liquid Metal Rankine Topping Cycle for a Steam Power Plant," *Journal of Spacecraft*, Vol. 4, pp. 859-964.

[13]Gregory, D. L., and Woodcock, G. R., *Solar Power Satellite, System Definition Study,* Vol. III, "SPS Satellite Systems," NASA-Johnson Space Center, Contract No. NAS9-1596, Dec. 1977.

[14]Zimmerman, W. F., "Alkali Metal Space Power Technology Applicable to National Energy Research and Development," *Journal of Energy*, Vol. 1, 1977, pp. 159-168.

[15]Elliot, D. G., "Rotary Radiators for Reduced Space Powerplant Temperatures," *Space Nuclear Power Systems,* Vol. 1, edited by M. S. El-Genk and M. D. Hoover, Robert E. Krieger Publishing Company, Inc., Melbourne, Australia, 1984.